Published in final edited form as:
J Hydrol (Amst). 2021 March 01; 594: 1–125720. doi:10.1016/j.jhydrol.2020.125720.

Comparison of recharge from drywells and infiltration basins: A modeling study

Salini Sasidharan[a,b], **Scott A. Bradford**[b], **Jiří Šimůnek**[a], **Stephen R. Kraemer**[c]

[a]Department of Environmental Sciences, University of California Riverside, Riverside, CA 92521, USA

[b]United States Department of Agriculture, Agricultural Research Service, U. S. Salinity Laboratory, Riverside, CA 92507, USA

[c]U.S. Environmental Protection Agency, Office of Research and Development, San Francisco, CA 94105, USA

Abstract

Drywells (DWs) and infiltration basins (IBs) are widely used as managed aquifer recharge (MAR) devices to capture stormwater runoff and recharge groundwater. However, no published research has compared the performance of these two engineered systems under shared conditions. Numerical experiments were conducted on an idealized 2D-axisymmetric domain using the HYDRUS (2D/3D) software to systematically study the performance of a circular IB design (diameter and area) and partially penetrating DW (38 m length with water table > 60 m). The effects of subsurface heterogeneity on infiltration, recharge, and storage from the DW and IB under constant head conditions were investigated. The mean cumulative infiltration (μI) and recharge (μR) volumes increased, and the arrival time of recharge decreased with the IB area. Values of μI were higher for a 70 m diameter IB than an DW, whereas the value of μR was higher for a DW after 1-year of a constant head simulation under selected subsurface heterogeneity conditions. A comparison between mean μI, μR, and mean vadose zone storage (μS) values for all DW and IB stochastic simulations (70 for each MAR scenario) under steady-state conditions demonstrated that five DWs can replace a 70 m diameter IB to achieve significantly higher infiltration and recharge over 20 years of operation. Additional numerical experiments were conducted to study the influence of a shallow clay layer by considering an IB, DW, and a DW integrated into an IB. The presence of such a low permeable layer delayed groundwater recharge from an IB. In contrast, a DW can penetrate tight clay layers and release water below them and facilitate rapid infiltration and recharge. The potential benefits of a DW compared to an IB include

CRediT authorship contribution statement

Salini Sasidharan: Conceptualization, Investigation, Methodology, Data curation, Software, Formal analysis, Validation, Visualization, Writing - original draft. **Scott A. Bradford:** Conceptualization, Software, Resources, Supervision, Project administration, Funding acquisition, Writing - review & editing. **Jiří Šimůnek:** Conceptualization, Software, Resources, Supervision, Project administration, Funding acquisition, Writing - review & editing. **Stephen R. Kraemer:** Project administration, Funding acquisition, Writing - review & editing.

Declaration of Competing Interest

The authors declare that they have no known competing financial interests or personal relationships that could have appeared to influence the work reported in this paper.

Appendix A. Supplementary data

a smaller footprint, the potential for pre-treatments to remove contaminants, less evaporation, less mobilization of in-situ contaminants, and potentially lower maintenance costs. Besides, this study demonstrates that combining both IB and DW helps to get the best out of both MAR techniques.

Graphical Abstract

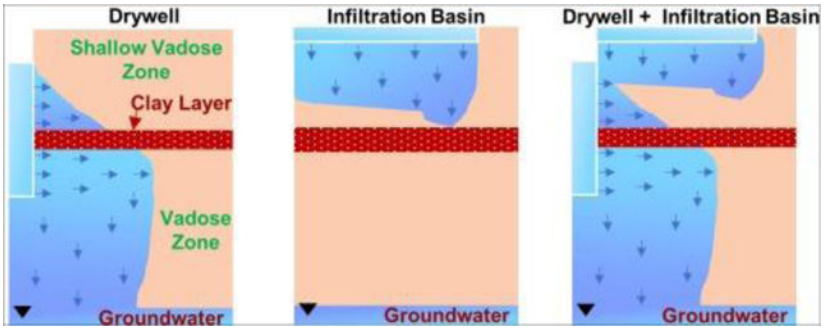

Keywords

Managed aquifer recharge (MAR); Drywell; Infiltration Basin; Infiltration; Recharge; HYDRUS (2D/3D)

1. Introduction

Climate models, combined with water budgets and socioeconomic information, suggest that a large proportion of the world's population is experiencing water stress (Vorosmarty et al., 2000). In recent decades, groundwater has been used as a freshwater resource when surface water is scarce (Famiglietti, 2014, Zektser and Lorne, 2004). However, intensive groundwater withdrawals have contributed to the depletion of streams (Fleckenstein et al., 2004), land subsidence, irreversible reduction of storage area (Faunt et al., 2016, Niswonger et al., 2017), drying up of pumping wells, increased cost of pumping from deep aquifers (Nelson et al., 2016), exacerbated seawater intrusion in coastal basins (Harter, 2015, Niswonger et al., 2017), disconnected stream-aquifer systems (Dogrul et al., 2016), and compromised groundwater quality (Feng et al., 2013, Ghasemizade et al., 2019, Niswonger et al., 2017).

Stormwater has been increasingly integrated into sustainable urban water management plans and developments (Chang et al., 2018). Managed aquifer recharge (MAR) uses various cross-cutting technologies for the intentional diversion, transport, storage, infiltration, and recharge of excess surface water (Sprenger et al., 2017). For example, MAR can be accomplished using infiltration basins (IB) (Teatini et al., 2015), aquifer storage and recovery (Dillon et al., 1999), aquifer storage, transfer, and recovery (Pavelic et al., 2005), flooding land (Flood-MAR) (Scherberg et al., 2014), flooding agricultural land (Ag-MAR) (Niswonger et al., 2017), and vadose zone recharge devices such as stormwater disposal wells (McClanahan, 2006), vadose zone trenches (Heilweil et al., 2015), infiltration wells, pits, recharge shafts, or drywells (DW) (Bouwer, 2002, Liang et al., 2018, Sasidharan et al., 2018, Sasidharan et al., 2019, Sasidharan et al., 2020). MAR has been expanding in

popularity and intensity to improve groundwater resources (Dillon et al., 2010, Ghasemizade et al., 2019).

The development of urban areas increases the impermeable surface area and the amount of runoff. Stormwater runoff threatens urban infrastructures (bridges, roads, and buildings) and wastewater treatment facilities, while contaminants associated with impervious surfaces (including fossil fuels, nutrients, and heavy metals) can impair surface water and groundwater quality (Welker et al., 2006). The elevated volume of surface runoff, therefore, has an adverse impact not only on the ecology and health of local rivers and streams but also has environmental effects miles downstream due to flooding, erosion, sediments, and contaminants (Braga et al., 2007). To tackle this problem, engineers are investing time, money, and research to develop Best Management Practices (BMPs) (Welker et al., 2006). Infiltration structures, such as infiltration basins and trenches, coupled with retention compartments, are widely used for urban stormwater management across the world (Dechesne et al., 2004, Dechesne et al., 2005).

Infiltration basins contribute valuable technical and environmental benefits by capturing stormwater runoff and letting it infiltrate into the underlying soil (Ferguson, 1994). They are an especially attractive and feasible option when the surface soil has adequate permeability, and the site has a shallow water table (Akan, 2002). Often, IBs drain runoff from mixed watersheds that have residential, commercial, and industrial zones, major roads, and reclaimed water (Dechesne et al., 2004, Drewes and Fox, 1999). The use of IBs enhances groundwater recharge, reduces the peak flow and volume of water in downstream networks, limits pollution discharges to surface waters, and decreases stormwater flows in sewer systems (Dechesne et al., 2004, Dechesne et al., 2005). Infiltration basins are also attractive to the public because they can improve urban landscapes when designed as parks or playgrounds. They have a lower cost than buried systems and act as drainage outlets from highways and parking lots (Dechesne et al., 2004, Dechesne et al., 2005).

Although there are many potential benefits associated with the use of IBs for stormwater capture, their more extensive application has certain limitations. For example, even though IBs are used as a stormwater management system in the urban area, it may not significantly decrease the total volume of runoff all the time (Traver and Chadderton, 1983). Therefore, they may not control potential flash flooding, erosion, and pollutants (Dechesne et al., 2005). Even though the topsoil layer of IBs can act as a barrier for pollutants (Mikkelsen et al., 1994, Nightingale, 1987), contamination of the underlying soil and groundwater still remains an issue (Barraud et al., 2002, Dechesne et al., 2004). In addition, clogging of IB surfaces (Barraud et al., 1999, Gonzalez-Merchan et al., 2012, Hutchinson et al., 2017) may occur through a combination of mechanical, biological, and chemical processes that depend on the sediment load and organic composition of the inflow water (Gonzalez-Merchan et al., 2012). Clogging reduces the infiltration capacity of IBs, and causes frequent ponding or overflows, reduces the treatment capacity, and decreases groundwater recharge (Dechesne et al., 2005, Gonzalez-Merchan et al., 2012). The annual cost associated with IBs maintenance, such as scrapping of clogged surfaces and pre-treatment of source water, can be expensive (Erickson et al., 2010). IBs can be operated for 20–30 years. However, the long-term performance of IBs is neither well understood nor controlled during operation (Dechesne

et al., 2005). Knowledge about the long-term environmental impacts of IBs is limited since there is no information on how to restore functionality if adequate infiltration capacity is lost (Welker et al., 2006). Also, there is a quantifiable decrease in the available area to operate IBs with increasing urbanization (Braga et al., 2007). There is, therefore, a critical need for alternative MAR practices that can resolve challenges associated with IBs in growing urban environments.

In the past decade, DWs have gained a lot of attention in the United States and across the world. DWs capture stormwater and infiltrate it in the vadose zone up to 10–40 m below the soil surface and at least 1–3 m above the water table (LACDPW, 2014, Sasidharan et al., 2018, Sasidharan et al., 2019, Sasidharan et al., 2020). DWs are often used as a Low Impact Development BMP engineering system to capture seasonal stormwater to maintain the urban green infrastructure. This study investigates the use of DWs for MAR as an alternative and/or in combination with IBs. DWs can be implemented as a MAR technique in semi-arid and arid regions where the groundwater table is deep (e.g., 60–300 m or more), when high permeable soils and/or sufficiently large land areas for surface infiltration systems are not available, or when the installation of deep boreholes in saturated zones are expensive (Bouwer, 2002, Liang et al., 2018). There are several additional advantages of using DWs over IBs. For example, DWs have minimal water loss by evaporation, a small installation area, a large ponding depth (hydraulic driving head), a shorter recharge time, and an opportunity for pre-treatment of sediments and contaminants in source water (Edwards et al., 2016, Sasidharan et al., 2018, Sasidharan et al., 2019, Sasidharan et al., 2020). A few major cities in California, Arizona, and Washington achieve nearly 70–100 percent of their groundwater recharge through DW infiltration, and many other cities are planning to build DWs (Cadmus, 1999, EPA, 1999, Graf, 2010, Marsh et al., 1995, Snyder et al., 1994). DWs are, therefore, an attractive option for MAR in areas where an IB is not ideal or can be used as an integrated infrastructure to enhance the recharge of existing IBs.

Several investigations have determined infiltration rates from infiltration basins (Bouwer, 2002, Bouwer and Rice, 1989, Masetti et al., 2016). In addition, several researchers have compared the performance of an IB with other MAR techniques. For example, lab-scale experiments coupled with numerical modeling have demonstrated that clogging is likely to influence the infiltration capacity of certain MAR systems (e.g., infiltration basins) more than others (e.g., recharge wells) (Glass et al., 2020). A small-diameter (2.5–5 cm diameter and 10–12 m depth) well was reported to improve the infiltration in comparison to a spreading basin (Händel et al., 2016a, Händel et al., 2014, Händel et al., 2016b). However, these studies used a small well that was not comparable to the drywell size of this investigation (1.2 m diameter and 38 m depth). Jokela and Kallio (2015) compared the performance of deep injection wells (40 cm diameter and 32–45 m depth) to a sprinkler infiltration system. Comparison between infiltration trenches and spreading basins demonstrated that trenches are promising to enhance infiltration when compared to spreading basins (Heilweil et al., 2015, Heilweil and Watt, 2011). In all of these studies, the well geometry was not identical to a drywell, and water was injected directly into the water table. Furthermore, differences in vadose zone storage and stochastic subsurface heterogeneity were not considered in these works.

MAR techniques are highly dependent on soil textural properties and the subsurface heterogeneity that controls both the permeability and flow fields. For example, the infiltration capacity will vary with the vadose zone thickness and the presence and distribution of high and low permeable soil layers and their connectivity to the underlying aquifer (Mantoglou and Gelhar, 1987, O'Geen et al., 2015, Schilling et al., 2017, Xie et al., 2014, Yeh et al., 1985a, Yeh et al., 1985b). Many parts of the US have soil horizons (layers) that are cemented or consist of claypans or layers with strongly contrasting particle size distributions. These layers can have exceptionally low saturated hydraulic conductivity (K_s) values that severely limit the vertical movement of infiltrated water (O'Geen et al., 2015). This restricts the site suitability and operation of IBs and does not guarantee that aquifer recharge from IBs will occur over short time frames (in some cases, it may be several years).

The objective of this study is to compare groundwater recharge from DWs and IBs under various homogeneous and heterogeneous subsurface conditions. The HYDRUS (2D/3D) software was used to directly simulate cumulative infiltration and recharge volumes from DWs and IBs. Constant head conditions were considered in DWs and IBs to determine the comparable upper limit for recharge. Subsurface heterogeneity was described in this model by generating stochastic realizations of soil hydraulic properties. The performance of DWs and IBs were assessed based on simulated values of cumulative infiltration and recharge, the number of DWs required to achieve similar or improved behavior to an IB, and the long-term operational benefits and costs. The approach and numerical model tool in this research can be used to screen MAR designs for a specific site applications.

2. Materials and methods

2.1. Mathematical model

The HYDRUS (2D/3D) software package version 3 (Šejna et al., 2018, Šimůnek et al., 2018, Šimůnek et al., 2016) was used to simulate infiltration, redistribution in the vadose zone, and groundwater recharge from DWs and IBs. HYDRUS (2D/3D) numerically solves the 2-dimensional axisymmetric form of the Richards equation using the van Genuchten (1980) and Mualem (1976) unsaturated soil hydraulic functions. Input parameters, initial conditions, and boundary conditions that were employed in these simulations were generally based on the results from DWs located in Fort Irwin, CA (Sasidharan et al., 2020). Table 1 provides a summary of hydraulic parameters that were employed in experiments I and II of this study, including the saturated soil hydraulic conductivity, Ks = 0.046 m day^{-1}; the shape parameter in the soil water retention function, α = 9.17 m^{-1}; the residual soil water content, θr = 0.043 [-]; the saturated soil water content, θs = 0.39 [-]; the pore-size distribution parameter in the soil water retention function, n = 2.76; and the tortuosity parameter in the hydraulic conductivity function, l = 0.5. In numerical experiments III (Table 1), default values of hydraulic parameters for various soil textural classes were taken from the HYDRUS (2D/3D) Soil Catalog (Carsel and Parrish, 1988).

The data for axisymmetric DW simulations presented in this work (one-year constant head simulation) was adapted from our previously published work, Sasidharan et al. (2020). This manuscript provides details about the expanded simulation domain, model parameters, and the dynamics of water infiltration, redistribution, and recharge. These results are compared

with similar simulations for IBs in this work. Fig. 1 shows a schematic of an example model domain, geometry, initial conditions, and boundary conditions that were employed in the IB simulations. The axisymmetric flow domain was 60 m (H, Height) × 50 m (W, Radius). The IB had a height of 2 m and a diameter of 10, 20, 30, 40, 50, 60, or 70 m, and was continuously ponded with a water height of 0.6 m. The model domain was discretized using a two-dimensional triangular finite element mesh with the MESHGEN tool available within HYDRUS (2D/3D). The mesh was refined at the top boundary of the domain, where infiltration from the IB was simulated. To reduce the mass balance error, the finite element mesh was adjusted such that the size of elements was smaller (0.05–0.1 m) near the IB surface, and the grid size was gradually increased with the radial distance from the IB, with a maximum element size of 0.5–0.75 m. The quality of the finite element mesh was assessed by checking the mass balance error reported by HYDRUS (2D/3D) at the end of the simulation. Mass balance errors were always below 1%, and these values are generally considered acceptable (Brunetti et al., 2017).

A no-flux boundary condition was assigned to nodes between the IB surface and the upper right corner, and the whole right and left sides of the flow domain (Fig. 1A). Nodes at the bottom boundary ($z = -60$ m) were assigned a free drainage boundary condition (i.e., the water table was assumed to be far below this point). Note that numerical experiments in this study do not account for the effect of the water table, and future site-specific analyses and modeling studies are therefore warranted. A constant pressure head condition was considered in this study to evaluate the continuous long-term performance of an IB, and potential application of a DW as an independent or integrated infrastructure with an IB. To represent a continuously filled IB (0.6 m), the total head ($H = h + z$) at the upper boundary (at $z = -1.4$ to -2 m) was constant, i.e., the pressure head decreased linearly with depth from 0.6 m at the bottom of the IB ($z = -2$ m) to 0 at the water level ($z = -1.4$ m) (Fig. 1). The initial condition in the flow domain was specified in terms of the soil water pressure head $h(x, z)$ and was set equal to a constant pressure head of −0.5 m (Fig. 1) (Sasidharan et al., 2020).

2.2. Numerical experiment

2.2.1. Homogeneous domain—Numerical experiments I (Table 1) were conducted to determine the values of cumulative infiltration (I) and cumulative recharge (R) after 730 days (2 years) as a function of the area of IB when considering a homogeneous Fort Irwin soil. The hydraulic parameters for the Fort Irwin soil (Table 1) were taken from Sasidharan et al. (2020). The value of I was collected over simulated time as the total volume of water infiltrated from the IB. Similarly, the value of R was calculated as the total volume of water drained through the bottom free drainage boundary. Note that all this information was available in output files of the HYDRUS (2D/3D) software.

2.2.2. Heterogeneous domain—Numerical experiments I considered idealized homogeneous soil systems. However, most field-scale soil profiles are highly heterogeneous, with hydraulic parameters changing over short distances. In this study, highly permeable horizontal and vertical soil layers/lenses were represented using the Miller-Miller similitude geostatistical approach, which has been widely used in previous research (Feyen et al.,

1998, Roth, 1995, Roth and Hammel, 1996, Sasidharan et al., 2019, Sasidharan et al., 2020, Vereecken et al., 2007). The HYDRUS (2D/3D) computer software has an option to generate stochastic distributions of hydraulic conductivity (α_K) and pressure head (α_h) scaling factors using the Miller-Miller similitude approximation (Miller and Miller, 1956), which links these two scaling factors as follows: $\alpha_K = \alpha_h^{-2}$. A lognormal distribution of scaling factors was employed, and the stochastic field was generated using the standard deviation (σ) of $\log_{10}(\alpha_K)$, and its correlation length in the lateral (the X-correlation length, X) and vertical (the Z-correlation length, Z) directions. Procedures for generating autocorrelated or uncorrelated scaling factor fields and the original algorithm used in HYDRUS have been described in detail in the literature (El-Kadi, 1986, Freeze, 1975, Mejía and Rodríguez-Iturbe, 1974).

Constant head IB simulations that employed stochastic realizations were conducted to accurately capture and compare the infiltration and recharge behavior of IBs with published constant head stochastic DW simulations (Sasidharan et al., 2020). Soil hydraulic parameters for the Fort Irwin soil (Table 1) were employed in conjunction with stochastic scaling factors in these simulations. Constant head simulations were used to determine I and R after two years in experiment II (Table 1). Multiple realizations of the stochastic parameters were employed, and the mean values of I (μI) and R (μR) and associated standard deviations were calculated. The following hypothetical combinations of scaling factors with variable σ (σ = 0.25,0.5, and 1 for X = 1 m and Z = 0.1m), X (X = 0.1, 1, and 10 m for σ = 1 and Z = 0.1 m), and Z (Z = 0.1, 1, and 2 m for σ = 1 and X = 1) were used. Similar parameter ranges have been measured in the field (Freeze, 1975, Sudicky and MacQuarrie, 1989) and employed in previous modeling studies (Sasidharan et al., 2019, Sasidharan et al., 2020). Only ten realizations were considered for these stochastic heterogeneity parameter combinations to minimize the computational time and cost. Our previous research demonstrated that ten realizations were sufficient to accurately capture the mean and variance of the infiltration behavior of DWs in the heterogeneous realizations of the numerical experiments (Sasidharan et al., 2019, Sasidharan et al., 2020). Mean parameter values and 95%-Confidence Intervals (CI) were calculated for all parameters from the ten simulation realizations of the IB after two years. The calculated values of μI and μR for IBs were compared with those for DWs (Sasidharan et al., 2020) with the same heterogeneous domain after 1 year.

We also compare the steady-state performance of a combined system with a 70 m diameter IB and a DW over two years in order to develop recommendations on how a DW can replace or complement an IB. Figure S1 demonstrates that the steady-state infiltration (i) and recharge (r) rates were reached in constant-head DW (Sasidharan et al., 2020) and IB simulations after one and two years, respectively. These values of i and r were multiplied by a selected duration to determine the total steady-state volume of I and R, respectively, after two years. The corresponding steady-state volume change of water in storage (S) in the vadose zone was determined as I-R. Steady-state values of μI, μR, and μS, and their associated 95% confidence intervals over a two-year duration were determined and compared for all DW and IB simulations (70 simulations for each MAR approach). Steady-state IB results were also compared with multiple DWs (up to 5) over 20 years of operation. In this case, values of μI, μR, and μS for two years were divided by two to obtain yearly

results and then multiplied by the number of years of operation and the number of DWs. Parameters μI^*, μR^*, and μS^* denote mean cumulative infiltration, recharge, and storage, respectively, under steady-state conditions using the 70 simulations.

As discussed in the introduction, fine-textured soil layers can lead to reductions in soil permeability and recharge. Additional simulations were, therefore, conducted to investigate the use of various MAR strategies to overcome these challenges in a profile with sand, loamy sand, sandy loam, sandy clay loam, and clay layers (Experiment III, Table 1). Soil hydraulic parameters for various soil textures were taken from the HYDRUS (2D/3D) Soil Catalog (Table 1). MAR simulations considered a single DW and IB separately, as well as a DW integrated into an IB (Fig. 1B and S2).

2.2.3. Cost-analysis for DW and IB—A brief economic analysis of the installation and operational costs of IBs and DWs was also conducted. Literature values and data collected from various commercial operators were used for this purpose.

3. Result and discussions

3.1. Performance of an IB in different soil profiles

The infiltration, recharge, and vadose zone storage volume for an IB with a diameter of 10–70 m were investigated as a function of time (1–2 years) and depth (7–60 m) using HYDRUS (2D/3D) numerical modeling experiments. Selected numerical experiments were conducted for homogeneous and stochastic (Fort Irwin) soil profiles to understand the effect of subsurface soil heterogeneity on IB performance.

3.1.1. Homogeneous soil profiles—Numerical experiment I was conducted to better understand the relationship between the size and the infiltration and recharge behavior of an IB in a homogeneous soil domain. IBs with a diameter of 10, 20, 30, 40, 50, 60, and 70 m were considered in this study. It should be mentioned that some existing IBs are much larger (1000 acre = 4 million m^2) and can infiltrate up to 308 million m^3 of water (Hutchinson et al., 2017). However, this work only considers a small IB with a maximum diameter of 70 m in order to minimize the computational time and cost associated with simulations on larger flow domains, and to stay within the empirical experience (catchment basin size) at the Fort Irwin study site. Fig. 2 shows the simulated water content (θ) profiles for IBs of different sizes after a 2-year, constant head, numerical simulation. Fig. 3, Fig. 4 present corresponding information about I and R in these same simulations. Fig. 3A shows a plot of I versus time for two years (730 days) of numerical simulation. Fig. 3B shows a plot of I versus the IB area after one and two years. The value of I increases in nearly a linear fashion over time (Fig. 3A) and with the IB area (Fig. 3B).

The design and operation standards for IBs are set by various states and counties. For example, in Virginia, the maximum drainage area of an IB is restricted to 50 acres, and the basin should be emptied within 48 h (Yu and Kaighn, 1992). In contrast, Los Angeles County in California requires that the 85th percentile of a 24-hr runoff event be infiltrated within 96 h (LACDPW, 2014). However, acquiring the needed land area for an IB can be expensive and challenging, especially in an urban area. Engineers, therefore, often seek

ways to minimize the surface area of an IB, but this can be challenging because it may require a ponding depth that is either impractical or violates design parameters. Besides, the actual configuration of an IB is largely dependent on the site-specific topography and other constraints (Yu and Kaighn, 1992). IBs may, therefore, not be an ideal BMP or MAR technique when suitable locations are not readily available, such as in highly urbanized landscapes with utilities, in karst areas, and when surface slopes are higher than 20 percent (Yu and Kaighn, 1992).

Fig. 4A, 4B, 4C, and 4D show plots of cumulative recharge R as a function of time (over one year) and depth when the IB diameter was equal to 10, 30, 50, and 70 m, respectively. The value of R was negligible for all IBs with a 60 m deep soil profile during the first year. This happens because most of the infiltrating water below the IB contributes to the change in the vadose zone storage until the pore space is filled. The size of the IB influences the arrival time of the infiltrating water at a specified depth. In particular, a decrease in the IB diameter produced a later arrival time. For example, the arrival time at a depth of 22 m for an IB with a 10 m diameter was 164.8 days, whereas it was 126.8 days when the IB diameter was 70 m. This occurs because lateral spreading plays a relatively more significant role for smaller diameter IBs (Fig. 2).

Fig. 4E shows a plot of R as a function of the IB area at depths of 7, 22, and 60 m after one and two years. The value of R was very small or negligible after one year when the depth was 60 m, but then rapidly increased when the vadose zone storage filled, and the simulation approached a steady-state condition at the end of the second year. For example, the value of R at a depth of 60 m after 2 years was slightly less than R at a depth of 7 m after 1 year (Fig. 4E). This reflects the difference in the vadose zone storage and the time needed to reach steady-state conditions at these depths. It also indicates that IBs may not be the ideal MAR strategy when rapid groundwater recharge is needed. For example, the Central Valley in California is one of the most productive agricultural regions in the world, which heavily relies on surface water diversions and groundwater pumping for crop irrigation (Faunt et al., 2016). Greater reliance on groundwater during droughts has caused large scale land subsidence (Harter, 2015), and the loss of up to 10 m of aquifer storage in some parts of the Central Valley (Scanlon et al., 2016). Rapid recharge within a short period is, therefore, essential for mitigating land subsidence and irreversible loss in aquifer storage in shallow aquifers (60–70 m). However, our experiment I simulation results demonstrate that the IB design will determine the arrival time for groundwater recharge. In some cases, this may take several years, even for a homogeneous soil profile with high permeability.

3.1.2. Heterogeneous soil profiles—In reality, the natural subsurface is inherently heterogeneous, and the layering of soil structures is very common (Hencher et al., 2011, Phillips and Lorz, 2008, Sasidharan et al., 2019, Sidle et al., 2000, Smith et al., 2008, Uchida et al., 2003, USDA, 2016). Fig. 5 shows representative θ distributions in stochastic domains under a 70 m diameter IB that had constant head conditions for two years. The Fort Irwin soil hydraulic parameters and stochastic parameters X = 0.1, 1, and 10; Z = 0.1, 1, and 2; and σ = 0.25, 0.5, and 1 were employed in these experiment II simulations (Table 1). Heterogeneous domains with X = 10, 1, and 0.1 (lateral layering, Fig. 5A, 5B, and 5C) display wider θ distributions in the saturated area under the IBs compared to

other heterogeneous domains. However, constant head simulation results indicate that a DW (Sasidharan et al., 2020) with a 1.8 m diameter can create a similar-sized cone of infiltration as a 70 m diameter IB (Fig. S3). The operation of IBs is mainly controlled by gravity-driven vertical water flow, but the pressure head for an IB is very small (0.6 m). In contrast, a DW can have a pressure head of up to 38 m that pushes water initially laterally through high permeable zones, and then water flows vertically by gravity. Therefore, a DW with a very small surface footprint can create a recharge zone as big as a 70 m diameter IB. In particular, the surface area of a 70 m IB is 3857 m^2, whereas it is only 2.54 m^2 for a DW.

Fig. 6 shows values of μI and μR, and their 95% confidence intervals after 365 days as a function of σ (Fig. 6A), X (Fig. 6B), and Z (Fig. 6C) for the DW (Sasidharan et al., 2020) and IB. Sasidharan et al. (2020) previously demonstrated in DW simulations that the infiltration volume, the distribution and volume of trapped water in the flow domain, and the subsequent recharge are highly dependent on the subsurface heterogeneity. Similarly, Fig. 6A shows that μI and μR tended to increase with σ (Fig. 6A) for both IB and DW. An increase in σ leads to the formation of more permeable regions, which enhance infiltration (Sasidharan et al., 2020). The μI was higher for the IB than for the DW, but μR for the IB was smaller than for the DW. The value of μI and μR for the IB and DW overlapped for X (Fig. 6B), and in some cases μI and μR were higher for the DW than for the IB. In contrast, the value of μI was higher and μR smaller for the IB in comparison with the DW for various Z (Fig. 6C). An increase in X and Z creates larger horizontal and vertical lenses that can enhance the rapid movement of the wetting front in horizontal and vertical directions, respectively (Sasidharan et al., 2019, Sasidharan et al., 2020). The above numerical modeling observations can be explained by differences in the vadose zone storage and the time to reach steady-state flow conditions. In general, the DW has less vadose zone storage and therefore reaches steady-state flow conditions faster than the IB (Fig. S3). Recharge from the IB is, therefore, smaller than from the DW in the short-term. Researchers have previously reported extensive lateral water movement but limited vertical water movement in different subsurface soil profiles (Mantoglou and Gelhar, 1987, Routson et al., 1979, Sinai et al., 1974, Yeh et al., 1985a, Yeh et al., 1985b).

It is important to understand the infiltration, recharge, and arrival time behavior during short-term DW and IB operations to identify the best technique to infiltrate or recharge water rapidly. Fig. S4 shows a plot of μI and μR as a function of time (365 days) for IB simulations when σ = 0.25, 0.5, and 1, and when X = 1 m and Z = 0.1 m. The value of μI and μR tended to increase with σ, but μR was orders of magnitude smaller than μI due to vadose zone storage. The value of μR was equal to zero after one year for the IB when σ = 0.25, whereas the recharge arrival time for a DW was approximately 100 days when σ = 0.25 (Sasidharan et al., 2020). Fig. S5 shows a plot of μI and μR for the IB when X = 0.1, 1, 10 m, Z = 0.1 m, and σ = 1. The values of μI and μR decreased with increasing X. These trends reflect increasing water spreading with X due to larger lenses in the lateral direction with high permeability (Sasidharan et al., 2020). The value of μR was again orders of magnitude smaller than μI due to the vadose zone storage. The arrival time for the worst-case recharge scenario (X = 10, Z = 0.1 m, and σ = 1) was approximately 250 days for the IB (Fig. S5B) compared to about 68 days for the DW (Sasidharan et al., 2020). Fig. S6 shows a plot of μI and μR as a function of time (365 days) for IB simulations when Z = 0.1, 1, and 2, X = 1 m,

and $\sigma = 1$. The presence of highly permeable vertical lenses facilitates the faster downward movement of water and, thus, an early arrival time (Sasidharan et al., 2020). However, even for the best-case recharge scenario ($X = 1$, $Z = 2$, and $\sigma = 1$), the arrival time for the IB was approximately 135 days (Fig. S6B), whereas it was only about 34 days from the DW (Sasidharan et al., 2020). The above results clearly demonstrate that DWs have a much faster recharge arrival time than IBs.

3.2. Performance comparison between IB and DW

An IB has several benefits when used as a MAR technique. However, the biggest constrain on the installation of an IB often is land availability, both in urban and rural areas. Direct injection wells such as Aquifer Storage and Recovery has gained attention as a solution to this problem. However, injection water needs to meet strict water quality standards before being injected, which are achieved using energy-intensive treatments, which makes this technique very expensive. Drywells usually are considered as a Low Impact Development (LID) BMP for capturing episodic stormwater, mostly in urban areas. However, this study proposes its potential use as a MAR under constant head conditions, where the installation and continuous operation of an IB are not feasible. Therefore, additional numerical experiments were conducted to compare the infiltration and recharge performance between a DW and an IB under various scenarios. The purpose of these specific simulations was to demonstrate the potential application of a drywell as an independent MAR technique in place of an IB, or its use in conjunction with existing IB infrastructure. Such a combination of a DW with an IB has never been systematically investigated before.

Section 3.1. demonstrated that a single DW could infiltrate and recharge less, equivalent, or more water than a 70 m diameter IB depending on specific subsurface heterogeneity conditions. Additional calculations were conducted in this section to compare the overall performance of multiple DWs and an IB. Fig. 7 shows plots of mean steady-state values of μI^*, μR^*, and μS^* for simulations with an IB and a DW (70 for each MAR scenario) in heterogeneous domains as a function of the number of DWs. The value of μI^* and μR^* for a 70 m diameter IB and a single DW were very close to each other (Fig. 7A and 7B). However, increasing the number of DWs at a location increases values of μI^* and μR^* over the IB correspondingly to their numbers. Interestingly, the value of μS^* for a single DW was smaller than that for an IB, but the 95%-CI for the vadose zone storage volume for five DWs overlapped that of a single IB. These results demonstrate that five DWs can easily replace a 70 m diameter (a surface area of 3847 m^2) IB to achieve significantly higher infiltration and recharge.

Additional calculations were conducted to compare the performance of five DWs with a 70 m diameter IB that was operated for up to 20 years (Fig. 8). The results demonstrate that five DWs can infiltrate and recharge significantly higher volumes of water than an IB even after 20 years of continuous operation. These results have important implications for MAR operations. IBs often require a large surface area to infiltrate source water within the recommended time to minimize flooding and ponding (LACDPW, 2014, Yu and Kaighn, 1992). The implementation of IBs as a BMP in urban areas is especially challenging due to the limited land availability. Fig. 7, Fig. 8 clearly demonstrate that the installation of up to 5

DWs with a minimal footprint can easily replace a 70 m diameter (surface of 3847 m^2) IB. DWs offer unique design opportunities to install such devices in places where space is very tight, such as parking lots, parks, and streets. Fig. 5, Fig. 7, Fig. 8 demonstrated that IBs require a large volume of water to saturate the vadose zone (μS^*) before recharge can occur. This leads to a significant loss when the source water is seasonal (stormwater, rainwater, and peak river flow) or expensive (recycled wastewater). A previous study on vadose zone trenches demonstrated that infiltration increased between parallel trenches with increasing spacing and number of trenches, and when trenches were continuously full (Heilweil et al., 2015). DW offers flexibility to install with adequate spacing between each unit to enhance the infiltration and recharge, even in urban areas. The presented numerical modeling tool can be used to predict the best distribution of DWs, and it can be done with high accuracy when the site-specific subsurface heterogeneity information is available.

IBs are generally considered as the MAR technique of choice to enhance aquifer recharge and achieve groundwater sustainability (Teatini et al., 2015). However, expected long-term declines in the groundwater level could result in compaction of fine-grained deposits, which causes land subsidence (Galloway et al., 1999). For example, land subsidence from groundwater pumping in the San Joaquin Valley of Central California began in the mid-1920 s, and by 1970 about 13500 km^2 of land had subsided more than 0.3 m (Bertoldi et al., 1991, Poland et al., 1975). The Sustainable Groundwater Management Act (SGMA) recognizes that groundwater is best managed at the local level due to variabilities in geographic, geologic, and hydrologic parameters. The SGMA provides 20 years to implement reliable groundwater management plans to achieve long-term groundwater sustainability (Faunt et al., 2016). There is, therefore, an urgency for rapid recharge of these depleted aquifers before the aquifer storage space is irreversibly lost. Maples et al. (2019), in their modeling study on the infiltration basin at Central Valley, CA, demonstrated that geologic heterogeneity plays a huge role in the arrival time of recharge at the water table. The recharge potential from an IB is highly dependent on subsurface geologic structure, with a nearly two orders-of-magnitude range of recharge across the domain. They suggested that networks of interconnected coarse-texture facies provide a pathway for rapid infiltration and that the fine-texture facies accommodate a substantial fraction of the total recharge volume, even for coarse-dominated sites (Maples et al., 2019). Similarly, this research demonstrates that it can take several years for an IB to begin recharging an aquifer, depending on its size and the subsurface heterogeneity and permeability. In contrast, DWs can rapidly achieve significant amounts of recharge in a shallow unconfined aquifer within a much shorter time frame.

Natural geologic processes in sedimentary basins tend to produce soil textural layers and lenses that form parallel to the soil surface. These layered soil profiles can often involve highly permeable sand layers followed by less permeable clay lenses with extensions and thicknesses of several tens to hundreds of meters (Phillips and Lorz, 2008). Numerical experiments III (Table 1) were therefore conducted to study the influence of a shallow clay layer under an IB on infiltration and recharge. A layered soil profile with sand, loamy sand, sandy loam, sandy clay, loam, and clay was considered in these simulations (Table 1). Fig. S2 shows an illustration of the simulation domain and soil layers when considering an IB, a DW, and a DW integrated into an IB (denoted as DB + IB). Independent IB and

DW scenarios were used to better understand the infiltration and recharge behavior in the layered soil profile with these two structures. In contrast, the DW + IB approach (Fig. 9B) allowed us to assess the potential benefits of this MAR system. Fig. 9A and 9B show the water content (θ) and pressure head (h) profiles, respectively, for all three flow domains after 1.5 days. The results demonstrate that once the moisture front reached the clay layer, water started spreading laterally. The effect of a low permeable soil layer on the infiltration rate and downward migration from an infiltration basin was previously demonstrated using numerical experiments (D'Aniello et al., 2019). This enhanced lateral movement of water in the clay layer can be attributed to the fact that at higher tension, the hydraulic conductivity of fine-textured materials can be higher than in coarse-textured materials, and water may prefer to spread laterally in a fine bed than to move vertically through coarser ones (Routson et al., 1979, Sasidharan et al., 2020). The presence of such geological formations under an IB could delay groundwater recharge from 1 to more than 100 years. In contrast, a DW that penetrates tight clay layers and releases water below them can facilitate rapid infiltration and recharge. A DW can, therefore, be an ideal engineering solution to use in conjunction with an existing IB or when planning a new MAR site when there are shallow clay layers, and recharge is the primary goal.

The average one-time installation cost of a drywell (MaxWell IV, TorrentResources, USA, Personal Communication, 2020) is between $28,000 and $35,000 US Dollar. The MaxWell Plus (TorrentResources, USA) drywell with additional pre-treatment can cost $38,000-$45,000 US Dollar or higher. The average yearly maintenance cost (vacuuming the sedimentation chamber to remove the debris and sediments) for one drywell is about $1,000 US Dollars per year. Since a drywell has a very small surface footprint, developers do not usually "lose" any land when installing a drywell. The land cost for a drywell can, therefore, be assumed to be nearly zero (DeJong, 2020). Consequently, the installation and operation of a drywell over 20 years can cost around $48,000-$65,000 US Dollar, whereas those for five drywells can cost up to $240,000-$325,000 US Dollar.

The Orange County Water District (OCWD) of California, USA implements extensive MAR programs using seasonal stormwater (185 million m^3 per year) and recycled water (123 million m^3 per year) for aquifer replenishment or recharge, seawater intrusion control, water quality protection and improvement (Hutchinson et al., 2017). The major cost associated with IBs is the acquisition of land, especially in highly urbanized areas with little available land. For example, the OCWD spent $4M US Dollars per ha in 2014 to purchase land for a groundwater spreading basin (Hutchinson et al., 2017). In addition, clogging of the recharge facility is the biggest hurdle to maximizing the capacity of existing infrastructure. A recent study conducted by the OCWD on a riverbed filtration system (RFS) demonstrated that this technique was highly effective in removing suspended solids in recharge water and increasing the recharge capacity of the receiving basin. However, the installation of an operational scale RFS at the site has an annualized cost of $5.1 M US Dollar (Hutchinson et al., 2017). Constraints on land availability and costs of land acquisition and maintenance, therefore, make it difficult to transfer these MAR techniques to other parts of the world, especially in developing countries.

4. Conclusions

Numerical simulations using HYDRUS (2D/3D) were conducted to evaluate the performance of an IB for infiltration and recharge under various design parameters (i.e., diameter and area) in a homogeneous soil domain. The infiltration and recharge from an IB increase in a linear fashion with the IB's area. However, the arrival time of recharge at a depth of 60 m increases with decreasing IB area. Therefore, installation of a large (greater than70 m diameter) IB is required when rapid recharge to a deep aquifer is essential.

Additional numerical simulations were conducted to evaluate the performance of a 70 m diameter IB and a 38 m deep DW for infiltration, recharge, and storage under various stochastic heterogeneity conditions. The water content profiles for the IB and DW systems showed that after a 2-year constant head simulation, the areas of infiltration and recharge were similar for both DW and IB. The result demonstrated that during the first year of operation, cumulative infiltration and recharge would be higher for a single DW than an IB under the same stochastic heterogeneity conditions. Additional comparisons between the mean cumulative infiltration and recharge volume from 70 stochastic simulations under steady-state conditions demonstrated that five DWs could easily replace a 70 m diameter IB to achieve significantly higher infiltration and recharge, with a comparatively smaller volume of water lost to storage. Benefits from drywells were most pronounced during the first couple of years but still held under steady-state conditions over 20 years of operation. Additional numerical experiments were conducted to understand the effect of a layered soil profile on DW, IB, and DW + IB performance. Results demonstrate that drywells could potentially be used in combination with an IB to bypass low permeability layers such as a claypan. Bypassing clay-rich layers can provide an additional benefit by preventing the mobilization of in-situ contaminants to groundwater. Additional field-scale research is warranted to assess the full implications of this practice on in-situ contaminant transport and groundwater quality.

A DW provides additional benefits over an IB. For example, the surface area for a 70 m IB is 3857 m^2, whereas it is only 2.54 m^2 for a DW. The acquisition of land for an IB operation can be expensive, or the availability of land that meets IB engineering criteria might be scarce in an urban area. In contrast, drywells in the urban area often look similar to a utility hole and do not obstruct the development or landscape of infrastructures such as parking lots, streets, or pavement. Furthermore, drywells have minimal or zero evaporative losses in comparison with an IB since all of its infiltration area is underground. Therefore, drywells may be more attractive than an IB, especially in highly urbanized arid and semiarid regions of the world. One of the biggest challenges in the continuous operation of IBs is the sedimentation of colloidal particles on the surface and the formation of a clogged surface layer, which requires a complete halt in operation and scrapping of the surface. IBs also require additional maintenance such as vector control, vegetation and landscape maintenance, and testing of sediments from IBs for the accumulation of toxins, metals, and hydrocarbons (CABMP-Handbook, 2003). In contrast, drywells offer an opportunity for pre-treatment of the source water before injecting it into a drywell without altering its operation efficiency. Therefore, DWs can potentially replace IBs when the operation of IBs is not ideal, or when DWs can be installed in conjunction with IBs to improve

their efficiency. This study provides new design considerations and applications for DWs in combination with IBs based on numerical modeling. Note that DWs are often considered as a BMP for periodically capturing stormwater for recharge under transient water flow conditions. However, this study considers the use of a DW as a MAR technique under constant head or continuous infiltration conditions. DWs also offer an opportunity to design a transient (falling head) MAR system by merely turning on or off the source water pipe to control the residence time for contaminant attenuation. However, field-scale validation and long-term monitoring are essential to demonstrate these potential benefits, and this will be explored in future projects.

Supplementary Material

Refer to Web version on PubMed Central for supplementary material.

Acknowledgment

Funding for this research was provided by the U.S. Environmental Protection Agency (US EPA) through an interagency agreement with the United States Department of Agriculture (EPA DW-012-92465401; ARS 60-2022-7-002). The views expressed in this article are those of the authors and do not necessarily represent the views or policies of the U.S. Environmental Protection Agency. The mention of commercial products does not constitute an endorsement. We thank the two anonymous reviewers whose comments/suggestions helped improve and clarify this manuscript.

References

Akan AO, 2002. Modified rational method for sizing infiltration structures. Can. J. Civ. Eng 29 (4), 539–542. 10.1139/l02-038.

Barraud S, Gautier A, Bardin J-P, Riou V, 1999. The impact of intentional stormwater infiltration on soil and groundwater. Water Sci. Technol 39 (2), 185.

Barraud S, Gibert J, Winiarski T, Bertrand-Krajewski JL, 2002. Impact of a storm infiltration drainage system on soil and groundwater: Presentation of the OTHU project. Water Sci. Technol 45 (3), 203–210. [PubMed: 11905441]

Bertoldi GL, Johnston RH, Evenson KD, 1991. Groundwater in the central valley. A summary report. US Government Printing Office, California.

Bouwer H, 2002. Artificial recharge of groundwater: hydrogeology and engineering. Hydrogeol. J 10 (1), 121–142. 10.1007/s10040-001-0182-4.

Bouwer H, Rice RC, 1989. Effect of Water Depth in Groundwater Recharge Basins on Infiltration. J. Irrig. Drain E-Asce 115 (4), 556–567. 10.1061/(ASCE)0733-9437(1989)115:4(556).

Braga A, Horst M, Traver RG, 2007. Temperature Effects on the Infiltration Rate through an Infiltration Basin BMP. J. Irrig. Drain Eng 133 (6), 593–601. 10.1061/(ASCE)0733-9437(2007)133:6(593).

Brunetti G, Šimůnek J, Turco M, Piro P, 2017. On the use of surrogate-based modeling for the numerical analysis of Low Impact Development techniques. J. Hydrol 548, 263–277. 10.1016/j.jhydrol.2017.03.013.

CABMP-Handbook, 2003. Infiltration basin In: Muncipal CSBH (Ed.). www.cabmphandbooks.com .

Cadmus, 1999. State-by-state notebooks compiling results from the class v underground injection control study. United States Environmental Protection Agency.

Carsel RF, Parrish RS, 1988. Developing joint probability distributions of soil water retention characteristics. Water Resour. Res 24 (5), 755–769. 10.1029/WR024i005p00755.

Chang N-B, Lu J-W, Chui TFM, Hartshorn N, 2018. Global policy analysis of low impact development for stormwater management in urban regions. Land Use Policy 70, 368–383. 10.1016/j.landusepol.2017.11.024.

D'Aniello A, Cimorelli L, Cozzolino L, Pianese D, 2019. The Effect of Geological Heterogeneity and Groundwater Table Depth on the Hydraulic Performance of Stormwater Infiltration Facilities. Water Resour Manage 33 (3), 1147–1166. 10.1007/s11269-018-2172-5.

Dechesne M, Barraud S, Bardin J-P, 2004. Spatial distribution of pollution in an urban stormwater infiltration basin. J. Contam. Hydrol 72 (1–4), 189–205. 10.1016/j.jconhyd.2003.10.011. [PubMed: 15240172]

Dechesne M, Barraud S, Bardin J-P, 2005. Experimental Assessment of Stormwater Infiltration Basin Evolution. J. Environ. Eng 131 (7), 1090–1098. 10.1061/(ASCE)0733-9372(2005)131:7(1090).

DeJong B, 2020. Torrance drywell engineering plan and cost. In: Sasidharan S. (Ed.), Torrent Resources, pp. 1.

Dillon P, Pavelic P, Sibenbaler X, Gerges N, Clark R, 1999. Development of new water resources by aquifer storage and recovery using stormwater runoff. International Water and Irrigation 19 (2).

Dillon P, Toze S, Page D, Vanderzalm J, Bekele E, Sidhu J, Rinck-Pfeiffer S, 2010. Managed aquifer recharge: Rediscovering nature as a leading-edge technology. Water Sci. Technol 62 (10), 2338–2345. 10.2166/wst.2010.444. [PubMed: 21076220]

Dogrul EC, Kadir TN, Brush CF, Chung FI, 2016. Linking groundwater simulation and reservoir system analysis models: The case for California's Central Valley. Environ. Modell. Software 77, 168–182. 10.1016/j.envsoft.2015.12.006.

Drewes JE, Fox P, 1999. Fate of natural organic matter (nom) during groundwater recharge using reclaimed water. Water Sci. Technol 40 (9), 241–248.

Edwards EC, Harter T, Fogg GE, Washburn B, Hamad H, 2016. Assessing the effectiveness of drywells as tools for stormwater management and aquifer recharge and their groundwater contamination potential. J. Hydrol 539, 539–553. 10.1016/j.jhydrol.2016.05.059.

El-Kadi AI, 1986. A computer program for generating two-dimensional fields of autocorrelated parameters. Ground Water 24 (5), 663–667. 10.1111/j.1745-6584.1986.tb03715.x.

EPA, 1999. The class V underground injection control study. United States Environmental Protection Agency, Office of Ground Water Drinking Water.

Erickson AJ, Gulliver JS, Kang JH, Weiss PT, Wilson CB, 2010. Maintenance for stormwater treatment practices. Journal of Contemporary Water Research & Education 146 (1), 75–82.

Famiglietti JS, 2014. The global groundwater crisis. Nature Clim Change 4 (11), 945–948. 10.1038/nclimate2425.

Faunt CC, Sneed M, Traum J, Brandt JT, 2016. Water availability and land subsidence in the central valley, California, USA. Hydrogeology Journal 24 (3), 675–684.

Feng W, Zhong M, Lemoine J-M, Biancale R, Hsu H-T, Xia J, 2013. Evaluation of groundwater depletion in North China using the Gravity Recovery and Climate Experiment (GRACE) data and ground-based measurements: Groundwater Depletion In North China. Water Resour. Res 49 (4), 2110–2118. 10.1002/wrcr.20192.

Ferguson BK, 1994. Stormwater infiltration. CRC Press.

Feyen J, Jacques D, Timmerman A, Vanderborght J, 1998. Modeling water flow and solute transport in heterogeneous soils: A review of recent approaches. J. Agric. Eng. Res 70 (3), 231–256. 10.1006/jaer.1998.0272.

Fleckenstein J, Anderson M, Fogg G, Mount J, 2004. Managing Surface Water- Groundwater to Restore Fall Flows in the Cosumnes River. J. Water Resour. Plann. Manage 130 (4), 301–310. 10.1061/(ASCE)0733-9496(2004)130:4(301).

Freeze RA, 1975. A stochastic-conceptual analysis of one-dimensional groundwater flow in nonuniform homogeneous media. Water Resour. Res 11 (5), 725–741. 10.1029/WR011i005p00725.

Galloway DL, Jones DR, Ingebritsen SE, 1999. Land subsidence in the United States, 1182. US Geological Survey.

Ghasemizade M, Asante KO, Petersen C, Kocis T, Dahlke HE, Harter T, 2019. An Integrated Approach Toward Sustainability via Groundwater Banking in the Southern Central Valley, California. Water Resour. Res 55 (4), 2742–2759. 10.1029/2018WR024069.

Glass J, Šimůnek J, Stefan C, 2020. Scaling factors in HYDRUS to simulate a reduction in hydraulic conductivity during infiltration from recharge wells and infiltration basins. Vadose zone j. 19 (1) 10.1002/vzj2.20027.

Gonzalez-Merchan C, Barraud S, Le Coustumer Sebastien, Fletcher T., 2012. Monitoring of clogging evolution in the stormwater infiltration system and determinant factors. European Journal of Environmental and Civil Engineering 16 (sup1), s34–s47. 10.1080/19648189.2012.682457.

Graf C, 2010. Drywells—one county's novel approach to stormwater management and disposal. Southwest Hydrology 9 (1), 22–23.

Handel F, Binder M, Dietze M, Liedl R, Dietrich P, 2016a. Experimental recharge by small-diameter wells: the Pirna, Saxony, case study. Environ Earth Sci 75 (10). 10.1007/s12665-016-5701-7.

Handel F, Liu G, Dietrich P, Liedl R, Butler JJ Jr., 2014. Numerical assessment of ASR recharge using small-diameter wells and surface basins. J. Hydrol 517, 54–63. 10.1016/j.jhydrol.2014.05.003.

Handel F, Liu G, Fank J, Friedl F, Liedl R, Dietrich P, 2016b. Assessment of small-diameter shallow wells for managed aquifer recharge at a site in southern Styria Austria. Hydrogeology Journal 24 (8), 2079–2091.

Harter T, 2015. California's agricultural regions gear up to actively manage groundwater use and protection. Cal Ag 69 (3), 193–201. 10.3733/ca.E.v069n03p193.

Heilweil VM, Benoit J, Healy RW, 2015. Variably saturated groundwater modeling for optimizing managed aquifer recharge using trench infiltration. Hydrol. Process 29 (13), 3010–3019.

Heilweil VM, Watt DE, 2011. Trench infiltration for managed aquifer recharge to permeable bedrock. Hydrol. Process 25 (1), 141–151. 10.1002/hyp.7833.

Hencher SR, Lee SG, Carter TG, Richards LR, 2011. Sheeting Joints: Characterisation, Shear Strength and Engineering. Rock Mech Rock Eng 44 (1), 1–22. 10.1007/s00603-010-0100-y.

Hutchinson AS, Rodriguez G, Woodside G, Milczarek M, 2017. Maximizing infiltration rates by removing suspended solids: Results of demonstration testing of riverbed filtration in orange county, California. Water, 9(2): 119.

Jokela P, Kallio E, 2015. Sprinkling and well infiltration in managed aquifer recharge for drinking water quality improvement in Finland. J. Hydrol. Eng 20 (3) 10.1061/(ASCE)HE.1943-5584.0000975.

LACDPW, 2014. Low impact development. County of Los Angeles Department of Public Works Los Angeles, USA.

Liang X, Zhan H, Zhang Y, 2018. Aquifer recharge using a vadose zone infiltration well. Water Resour. Res 54 (11), 8847–8863. 10.1029/2018WR023409.

Mantoglou A, Gelhar LW, 1987. Effective hydraulic conductivities of transient unsaturated flow in stratified soils. Water Resour. Res 23 (1), 57–67. 10.1029/WR023i001p00057.

Maples SR, Fogg GE, Maxwell RM, 2019. Modeling managed aquifer recharge processes in a highly heterogeneous, semi-confined aquifer system. Hydrogeology Journal 27 (8), 2869–2888.

Marsh FL, Dueker LL, Small GG, 1995. Recharge well technology at the water campus project, Scottsdale, Arizona. Artificial recharge of groundwater II. ASCE 220–230.

Masetti M, Pedretti D, Sorichetta A, Stevenazzi S, Bacci F, 2016. Impact of a storm-water infiltration basin on the recharge dynamics in a highly permeable aquifer. Water Resour Manage 30 (1), 149–165. 10.1007/s11269-015-1151-3.

McClanahan S, 2006. Stormwater pretreatment and disposal system. Google Patents.

Mejía Jose M., Rodríguez-Iturbe I, 1974. On the synthesis of random field sampling from the spectrum: An application to the generation of hydrologic spatial processes. Water Resour. Res 10 (4), 705–711. 10.1029/WR010i004p00705.

Mikkelsen PS, Weyer G, Berry C, Waldent Y, Colandini V, Poulsen S, Grotehusmann D, Rohlfing R, 1994. Pollution from urban stormwater infiltration. Water Sci. Technol 29 (1–2), 293–302.

Miller EE, Miller RD, 1956. Physical Theory for Capillary Flow Phenomena. J. Appl. Phys 27 (4), 324–332. 10.1063/1.1722370.

Nelson T, Chou H, Zikalala P, Lund J, Hui R, Medellín–Azuara J, 2016. Economic and water supply effects of ending groundwater overdraft in California's central valley. San Francisco Estuary and Watershed Science, 14(1).

Nightingale HI, 1987. Water quality beneath urban runoff water management basins. J Am Water Resources Assoc 23 (2), 197–205. 10.1111/j.1752-1688.1987.tb00797.x.

Niswonger RG, Morway ED, Triana E, Huntington JL, 2017. Managed aquifer recharge through off-season irrigation in agricultural regions: Managed aquifer recharge in agriculture. Water Resour. Res 53 (8), 6970–6992. 10.1002/2017WR020458.

O'Geen AT, Saal M, Dahlke H, Doll D, Elkins R, Fulton A, Fogg G, Harter T, Hopmans JW, Ingels C, Niederholzer F, Solis SS, Verdegaal P, Walkinshaw M, 2015. Soil suitability index identifies potential areas for groundwater banking on agricultural lands. Cal Ag 69 (2), 75–84. 10.3733/ca.v069n02p75.

Pavelic P, Dillon P, Robinson N, 2005. Modeling of well-field design and operation for an aquifer storage transfer and recovery (astr) trial, Pro IAH XXXI Congress:" New Approaches to Characterizing Groundwater Flow. Swets Zeitlinger Lisse 859–862.

Phillips JD, Lorz C, 2008. Origins and implications of soil layering. Earth Sci. Rev 89 (3–4), 144–155. 10.1016/j.earscirev.2008.04.003.

Poland JF, Ireland R, Lofgren B, Pugh R, 1975. Land subsidence in the San Joaquin Valley, California, as of 1972.

Roth K, 1995. Steady State Flow in an Unsaturated, Two-Dimensional, Macroscopically Homogeneous, Miller-Similar Medium. Water Resour. Res 31 (9), 2127–2140. 10.1029/95WR00946.

Roth K, Hammel K, 1996. Transport of conservative chemical through an unsaturated two-dimensional Miller-similar medium with steady state flow. Water Resour. Res 32 (6), 1653–1663. 10.1029/96WR00756.

Routson R, Price W, Brown D, Fecht K, 1979. High-level waste leakage from the 241-t-106 tank at Hanford, Rockwell International Corp.

Sasidharan S, Bradford SA, Šimůnek J, DeJong B, Kraemer SR, 2018. Evaluating drywells for stormwater management and enhanced aquifer recharge. Adv. Water Resour 116, 167–177. 10.1016/j.advwatres.2018.04.003. [PubMed: 30245542]

Sasidharan S, Bradford SA, Šimůnek J, Kraemer SR, 2019. Drywell infiltration and hydraulic properties in heterogeneous soil profiles. J. Hydrol 570, 598–611. 10.1016/j.jhydrol.2018.12.073.

Sasidharan S, Bradford SA, Šimůnek J, Kraemer SR, 2020. Groundwater recharge from drywells under constant head conditions. J. Hydrol 583, 124569. 10.1016/j.jhydrol.2020.124569.

Scanlon BR, Reedy RC, Faunt CC, Pool D, Uhlman K, 2016. Enhancing drought resilience withconjunctive use and managed aquifer recharge in California and Arizona. Environ. Res. Lett 11 (3), 035013. 10.1088/1748-9326/11/3/035013.

Scherberg J, Baker T, Selker JS, Henry R, 2014. Design of Managed Aquifer Recharge for Agricultural and Ecological Water Supply Assessed Through Numerical Modeling. Water Resour Manage 28 (14), 4971–4984. 10.1007/s11269-014-0780-2.

Schilling OS, Irvine DJ, Hendricks Franssen H-J, Brunner P, 2017. Estimating the Spatial Extent of Unsaturated Zones in Heterogeneous River-Aquifer Systems: Estimating unsaturated zones. Water Resour. Res 53 (12), 10583–10602. 10.1002/2017WR020409.

Sejna M, Simůnek J, Genuchten M.T.v., 2018. The HYDRUS software package for simulating two- and three-dimensional movement of water, heat, and multiple solutes in variably-saturated porous media, User Manual, Version 3.0. PC Progress, Prague, Czech Republic, pp. 322.

Sidle RC, Tsuboyama Y, Noguchi S, Hosoda I, Fujieda M, Shimizu T, 2000. Stormflow generation in steep forested headwaters: a linked hydrogeomorphic paradigm. Hydrol. Process 14 (3), 369–385. 10.1002/(SICI)1099-1085(20000228)14:3<369::AID-HYP943>3.0.CO;2-P.

Simůnek J, Sejna M, van Genuchten MT, 2018. New features of version 3 of the HYDRUS (2D/3D) computer software package. Journal of Hydrology and Hydromechanics 66 (2), 133–142. 10.1515/johh-2017-0050.

Simůnek J, van Genuchten MT, Sejna M, 2016. Recent developments and applications of the HYDRUS computer software packages. Vadose Zone J. 15 (7), 25. 10.2136/vzj2016.04.0033.

Sinai G, Zaslavsky D, Golany P, 1974. Influence of anisotropy in soil permeability on surface runoff. In: Faculty of Agric. Eng, Israel T. Haifa (Ed.).

Smith JJ, Hasiotis ST, Woody DT, Kraus MJ, 2008. Paleoclimatic Implications of Crayfish-Mediated Prismatic Structures in Paleosols of the Paleogene Willwood Formation, Bighorn Basin, Wyoming, U.S.A. J. Sediment. Res 78 (5), 323–334. 10.2110/jsr.2008.040.

Snyder DT, Morgan DS, McGrath TS, 1994. Estimation of groundwater recharge from precipitation, runoff into drywells, and on-site waste-disposal systems in the portland basin, Oregon and Washington, 92. US Department of the Interior, US Geological Survey.

Sprenger C, Hartog N, Hernandez M, Vilanova E, Grützmacher G, Scheibler F, Hannappel S, 2017. Inventory of managed aquifer recharge sites in Europe: Historical development, current situation and perspectives. Hydrogeology Journal 25 (6), 1909–1922.

Sudicky E, MacQuarrie K, 1989. The behavior of biodegradable organic contaminants in random stationary hydraulic conductivity fields. In: Kobus HE, Kinzelbach W. (Eds.), Contaminant Transport in Groundwater, International Symposium on Contaminant Transport in Groundwater, pp. 307–315.

Teatini P, Comerlati A, Carvalho T, Gütz A-Z, Affatato A, Baradello L, Accaino F, Nieto D, Martelli G, Granati G, Paiero G, 2015. Artificial recharge of the phreatic aquifer in the upper Friuli plain, Italy, by a large infiltration basin. Environ Earth Sci 73 (6), 2579–2593. 10.1007/s12665-014-3207-8.

Traver RG, Chadderton RA, 1983. The downstream effects of stormwater detention basins, 1983 International Symposium on Urban Hydrology. Hydraulics and Sediment Control 455–460.

Uchida T, Asano Y, Ohte N, Mizuyama T, 2003. Seepage area and rate of bedrock groundwater discharge at a granitic unchanneled hillslope:Seepage area and rate of bedrock groundwater. Water Resour. Res 39 (1) 10.1029/2002WR001298.

USDA, 2016. Ssm - ch. 3. Examination and description of soil profiles. In: Staff R.b.S.S.D (Ed.), Soil Training. Natural Resources Conservation Service, USDA.

Vereecken H, Kasteel R, Vanderborght J, Harter T, 2007. Upscaling hydraulic properties and soil water flow processes in heterogeneous soils. Vadose Zone J. 6 (1), 1–28.

Vorosmarty CJ, Green P, Salisbury J, Lammers RB, 2000. Global water resources: Vulnerability from climate change and population growth. Science, 289(5477): 284– 8. [PubMed: 10894773]

Welker AL, Gore M, Traver R, 2006. Evaluation of the long term impacts of an infiltration BMP.

Xie Y, Cook PG, Brunner P, Irvine DJ, Simmons CT, 2014. When Can Inverted Water Tables Occur Beneath Streams? Groundwater 52 (5), 769–774. 10.1111/gwat.12109 .

Yeh T-C, Gelhar LW, Gutjahr AL, 1985a. Stochastic Analysis of Unsaturated Flow in Heterogeneous Soils: 3. Observations and Applications. Water Resour. Res 21 (4), 465–471. 10.1029/WR021i004p00465.

Yeh T-C, Gelhar LW, Gutjahr AL, 1985b. Stochastic Analysis of Unsaturated Flow in Heterogeneous Soils: 1. Statistically Isotropic Media. Water Resour. Res 21 (4), 447–456. 10.1029/WR021i004p00447.

Yu SL, Kaighn RJ, 1992. Vdot manual of practice for planning stormwater management. Virginia Transportation Research Council.

Zektser IS, Lorne E, 2004. Groundwater resources of the world: And their use. UNESCO, IHP series on groundwater.

Highlights

- Infiltration and recharge increase with the area of an infiltration basin.
- The arrival time of recharge from a drywell is shorter than an infiltration basin.
- Five drywells can infiltrate and recharge more water than a 70 m diameter infiltration basin.
- The benefit of a drywell still holds after 20 years of steady-state operation.
- Low permeability subsurface layers can be bypassed using a drywell and infiltration basin combination.

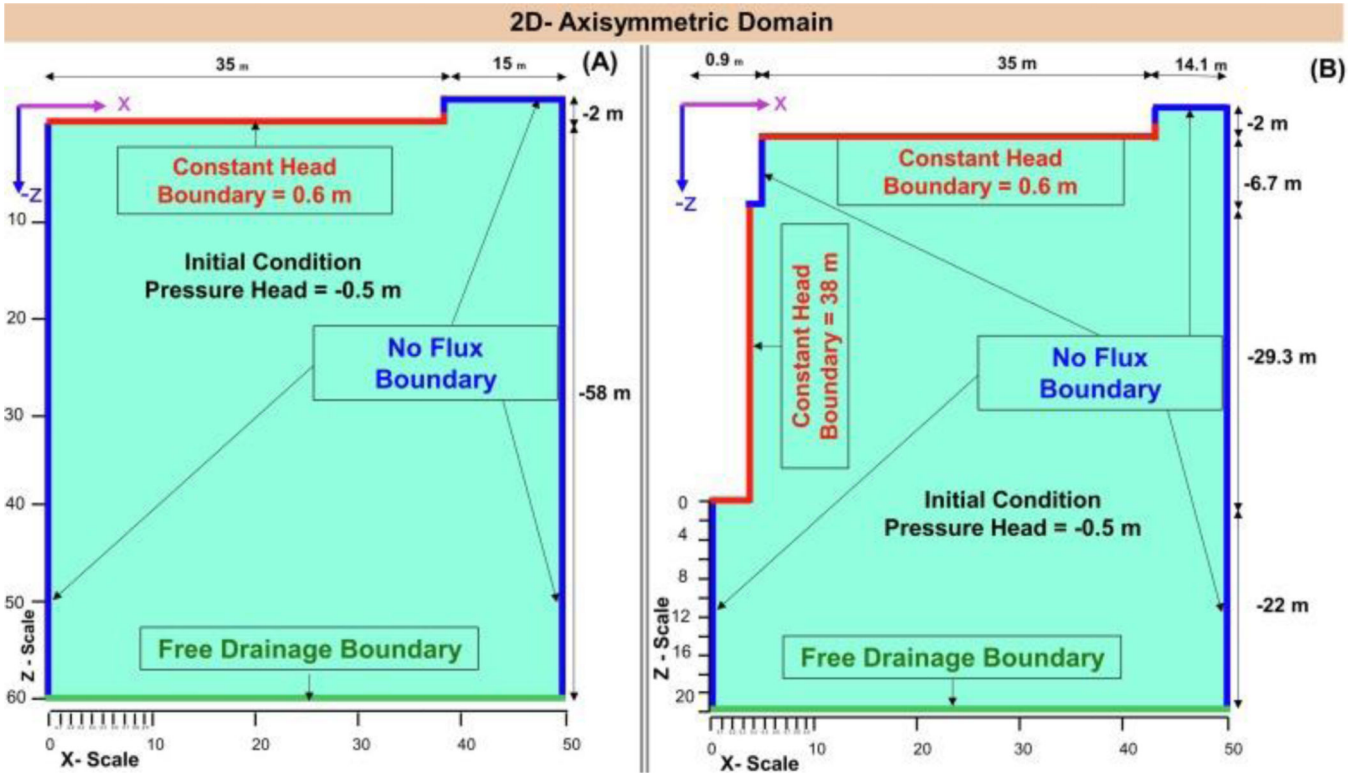

Fig. 1.

The geometry, dimensions, initial conditions, the boundary conditions, and X and Z directions for correlation length scales for the 2D-axisymmetrical infiltration basin (A) and DW + infiltration basin (B) flow domains. The detailed DW geometry, the water flow dynamics, and justification for initial and boundary conditions were presented in our previous studies (Sasidharan et al., 2018, Sasidharan et al., 2020).

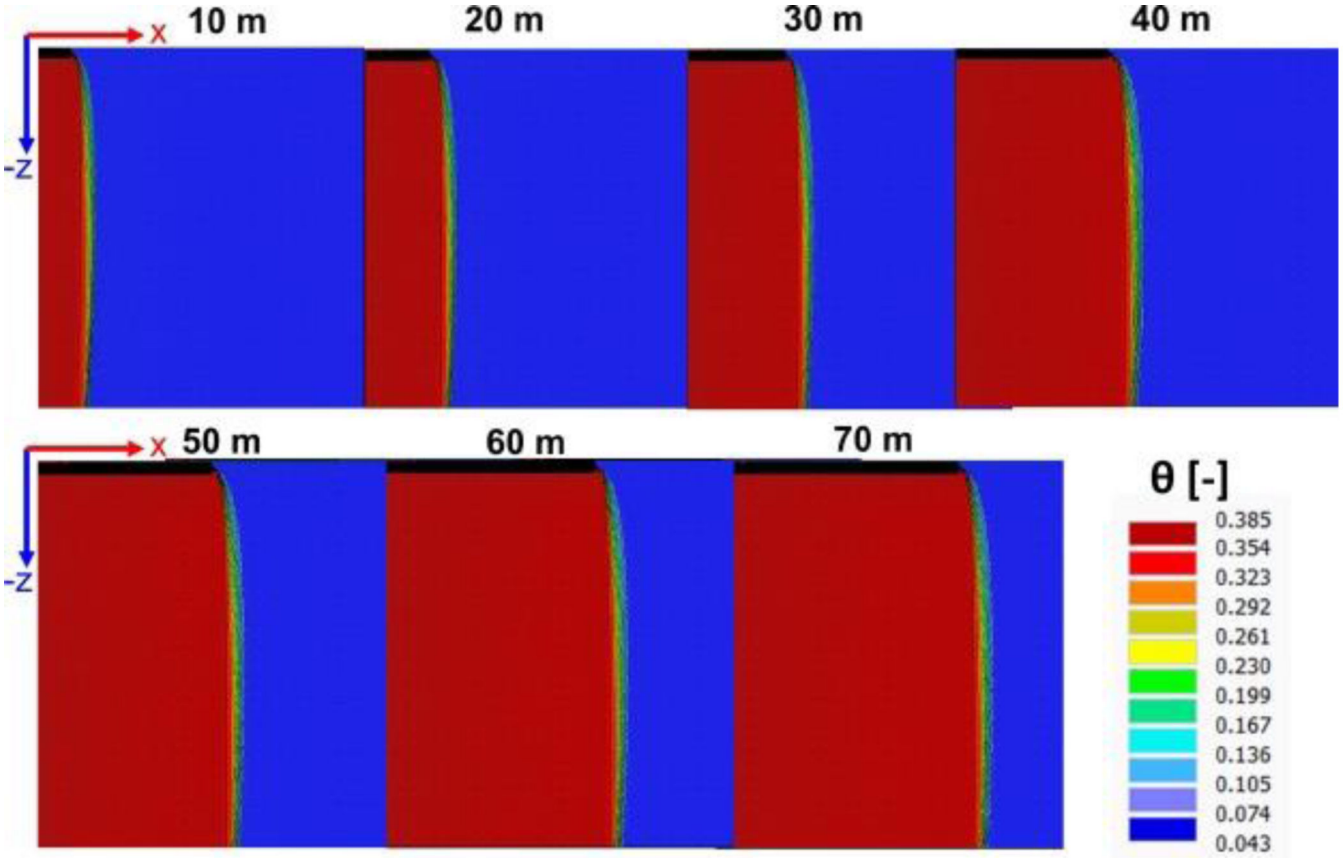

Fig. 2.

The cone of infiltration for a 10 m, 20 m, 30 m, 40 m, 50 m, 60 m, and 70 m diameter infiltration basins during a constant head simulation presented as water contents (θ) after two years of simulation.

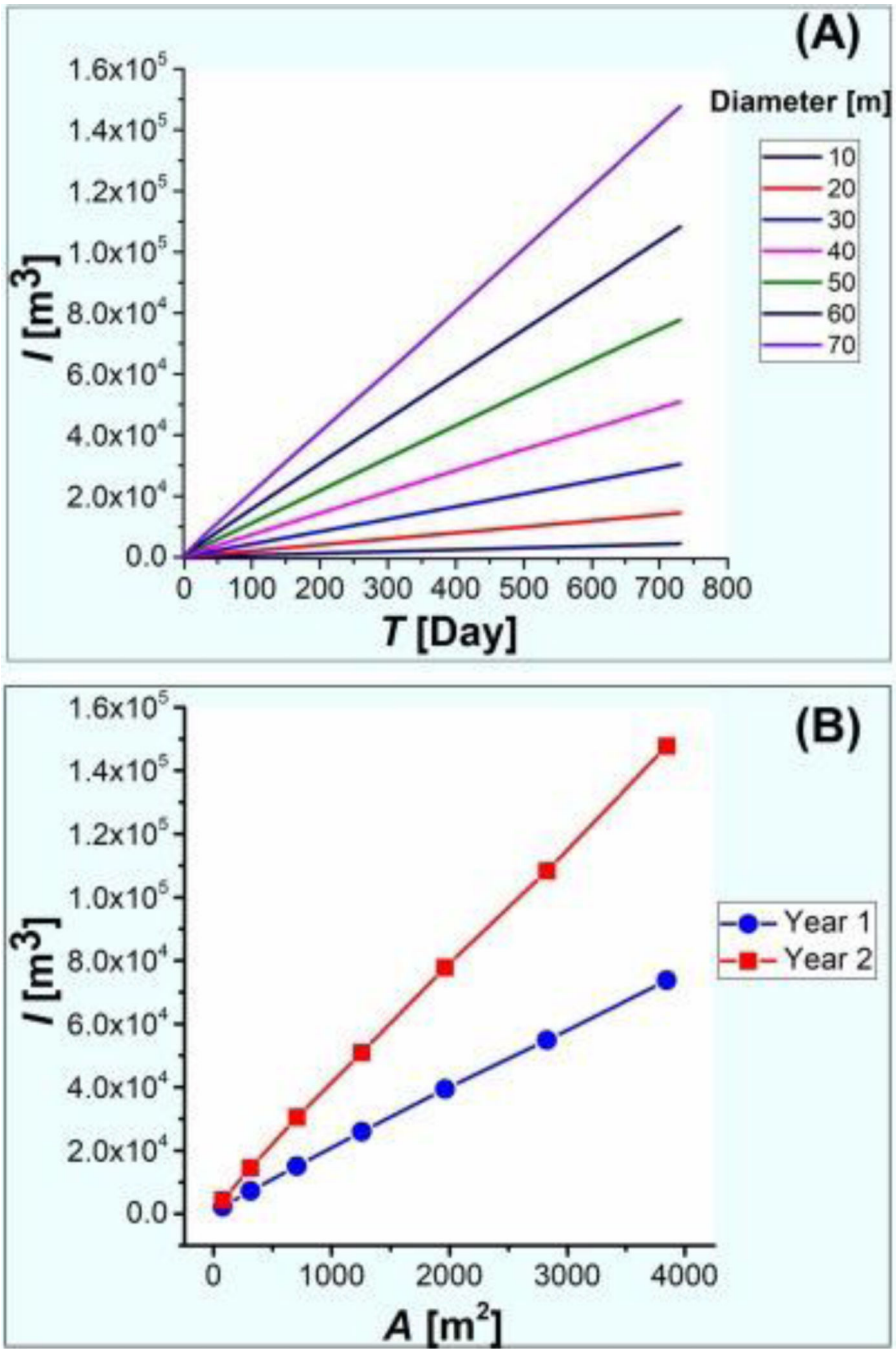

Fig. 3.

The cumulative infiltration volume (*I*) as a function of time (2 years or 730 days) (A) and the area of the infiltration basin (B).

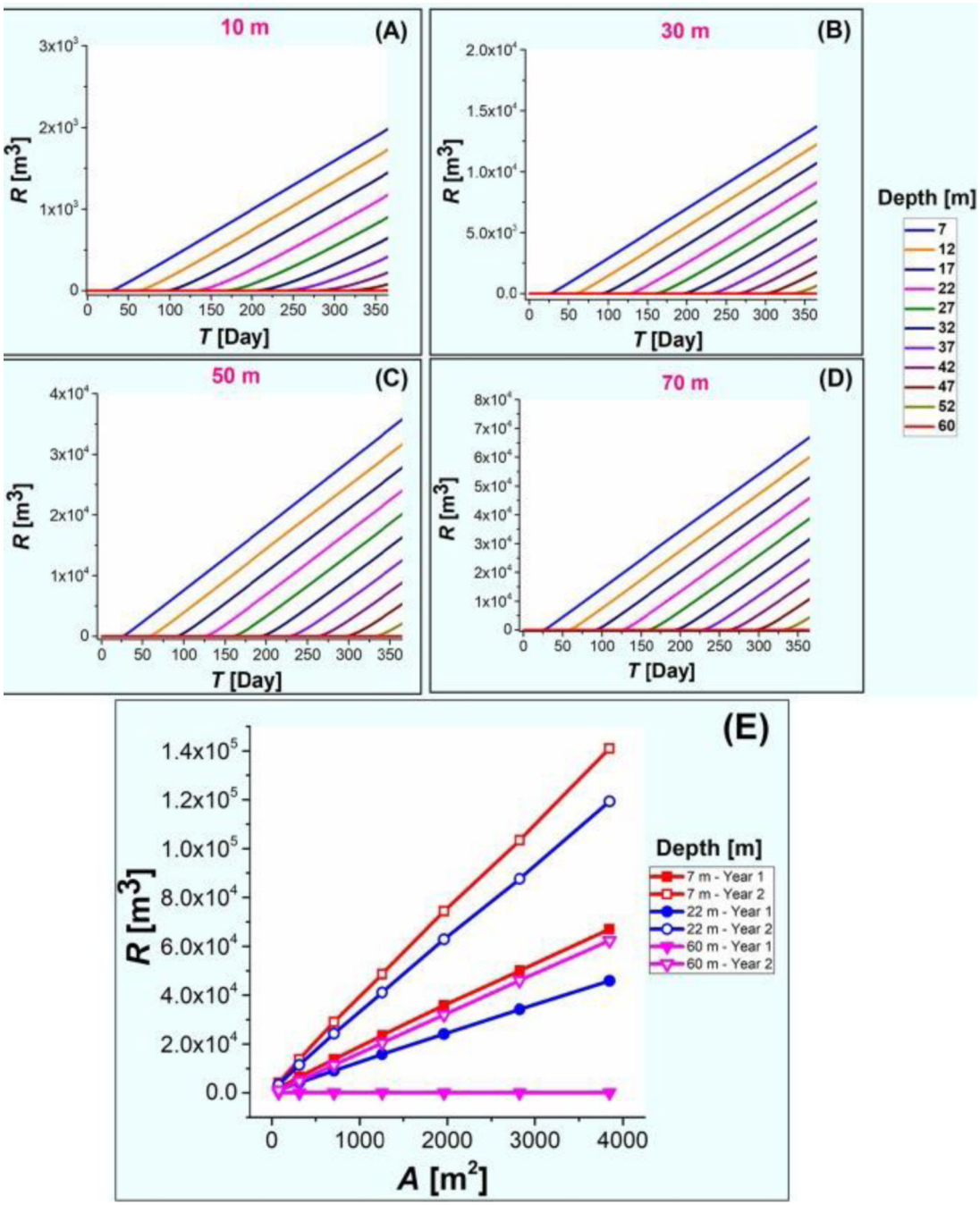

Fig. 4.

The cumulative recharge volume (*R*) at different depths as a function of time (1 year 365 days) for an infiltration basin with diameter = 10 m (A), 30 m (B), 50 m (C), and 70 m (D). The value of *R* as a function of the area of the infiltration basin at depths of 7 m, 22 m, and 60 m at Year 1 and Year 2 (E).

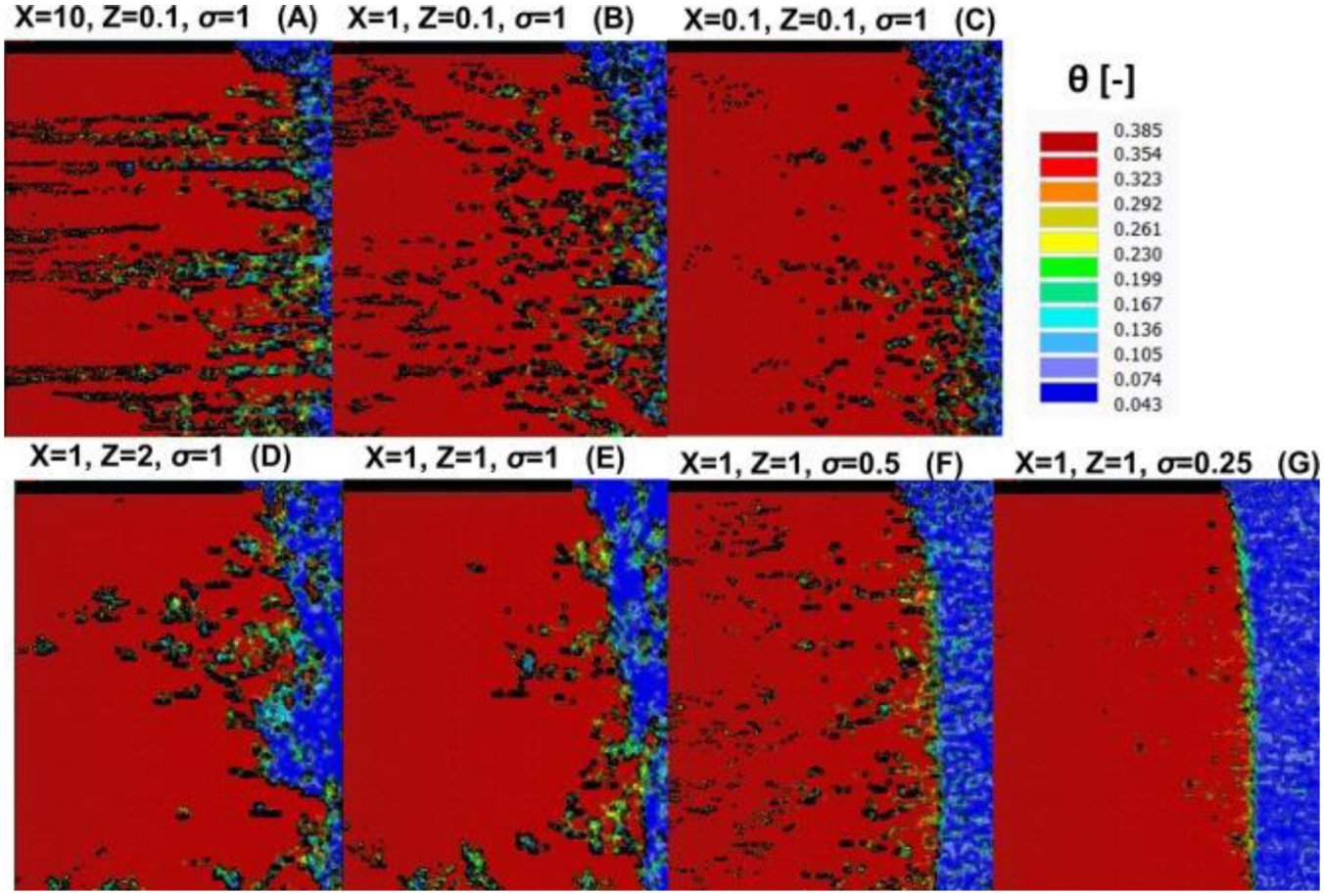

Fig. 5.

Water content (θ) profiles for heterogeneous Fort Irwin soil profiles after the 2-year constant head simulation. Heterogeneity parameters in these simulations were: (A) $X = 10$, $Z = 0.1$, $\sigma = 1$; (B) $X = 1$, $Z = 0.1$, $\sigma = 1$; (C), $X = 0.1$, $Z = 0.1$, $\sigma = 1$; (D), $X = 1$, $Z = 2$, $\sigma = 1$; (E), $X = 1$, $Z = 1$, $\sigma = 1$; (F), $X = 1$, $Z = 0.1$, $\sigma = 0.5$; and (G) $X = 1$, $Z = 0.1$, $\sigma = 0.25$.

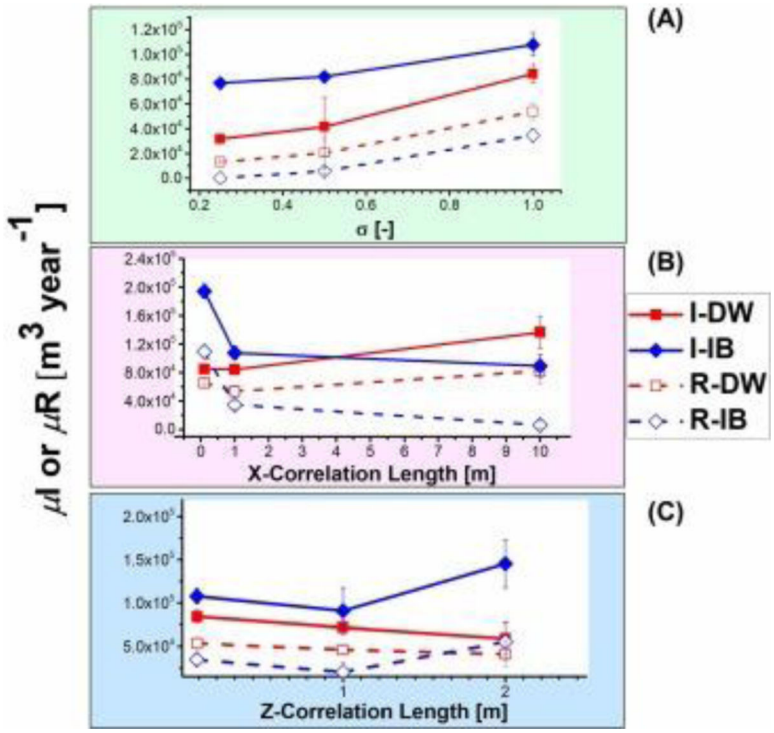

Fig. 6.

The mean cumulative infiltration volume (μI) and the mean cumulative recharge volume (μR) (from 10 simulations) and the corresponding 95% Confidence Intervals as a function of σ (σ = 0.25, 0.5, 1) when X = 1 and Z = 0.1 (A), X (X = 0.1, 1, 10 m) when σ = 1 andZ = 0.1 (B), and Z (Z = 0.1, 1, 2 m) when σ = 1 and X = 1 (C) for a heterogenous Fort Irwin soil flow domain with an IB or DW (Sasidharan et al., 2020) after 1-year constant head simulation.

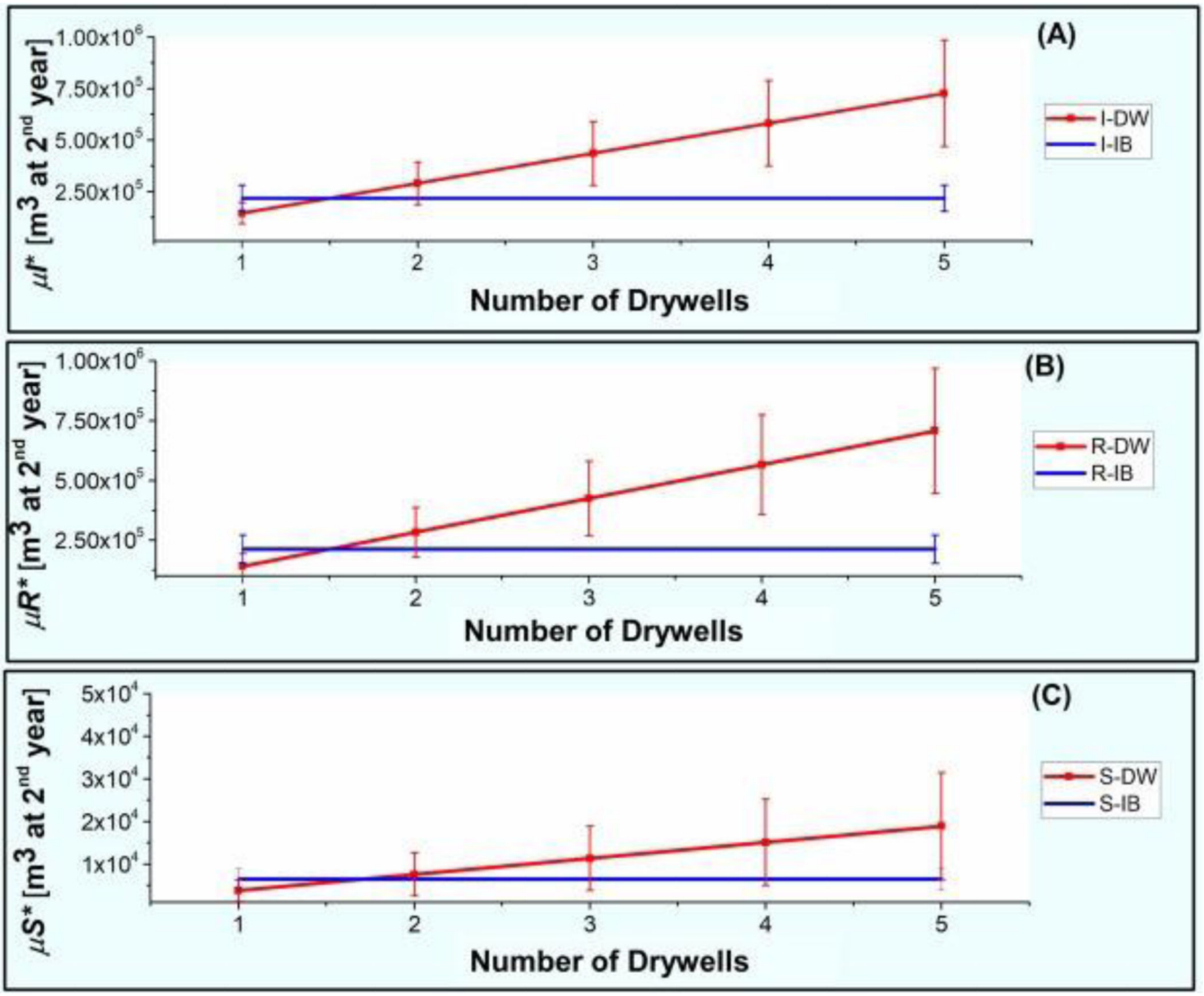

Fig. 7.

The mean cumulative infiltration volume (μI^*) (A), the mean cumulative recharge volume (μR^*) (B), and the mean cumulative storage volume (μS^*) (C) (from 70 simulations) as a function of the number of DWs (solid red line) after 2-year constant head simulations for the Fort Irwin soil flow domain. The solid blue line represents the corresponding value for a 70 m diameter infiltration basin (IB).

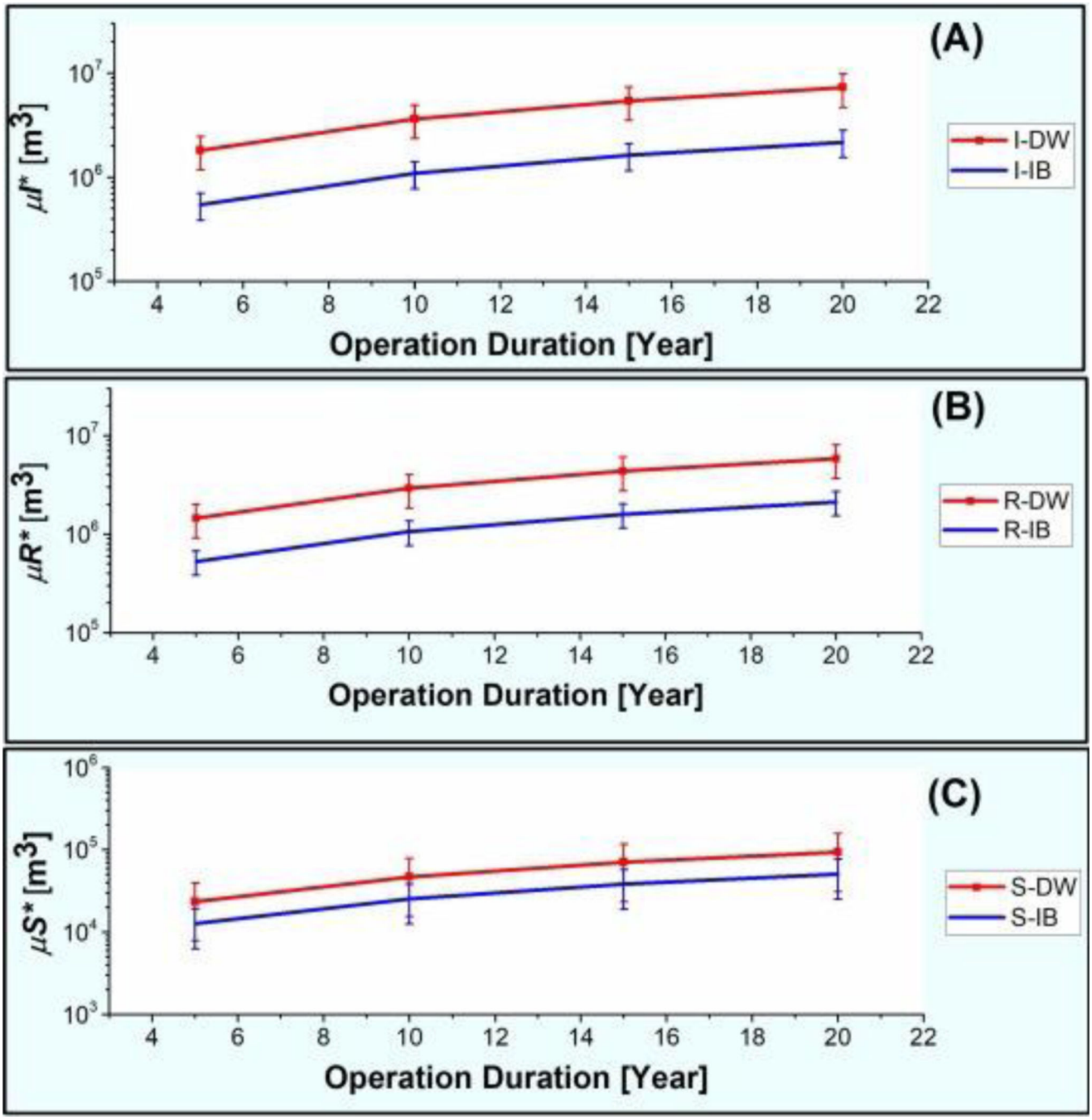

Fig. 8.

The mean cumulative infiltration volume (μI^*) (A), the mean cumulative recharge volume (μR^*) (B), and the mean cumulative storage volume (μS^*) (C) (from 70 simulations) as a function of operation duration for five DW (solid red line) and a 70 m diameter infiltration basin (solid blue line) for the Fort Irwin soil flow domain.

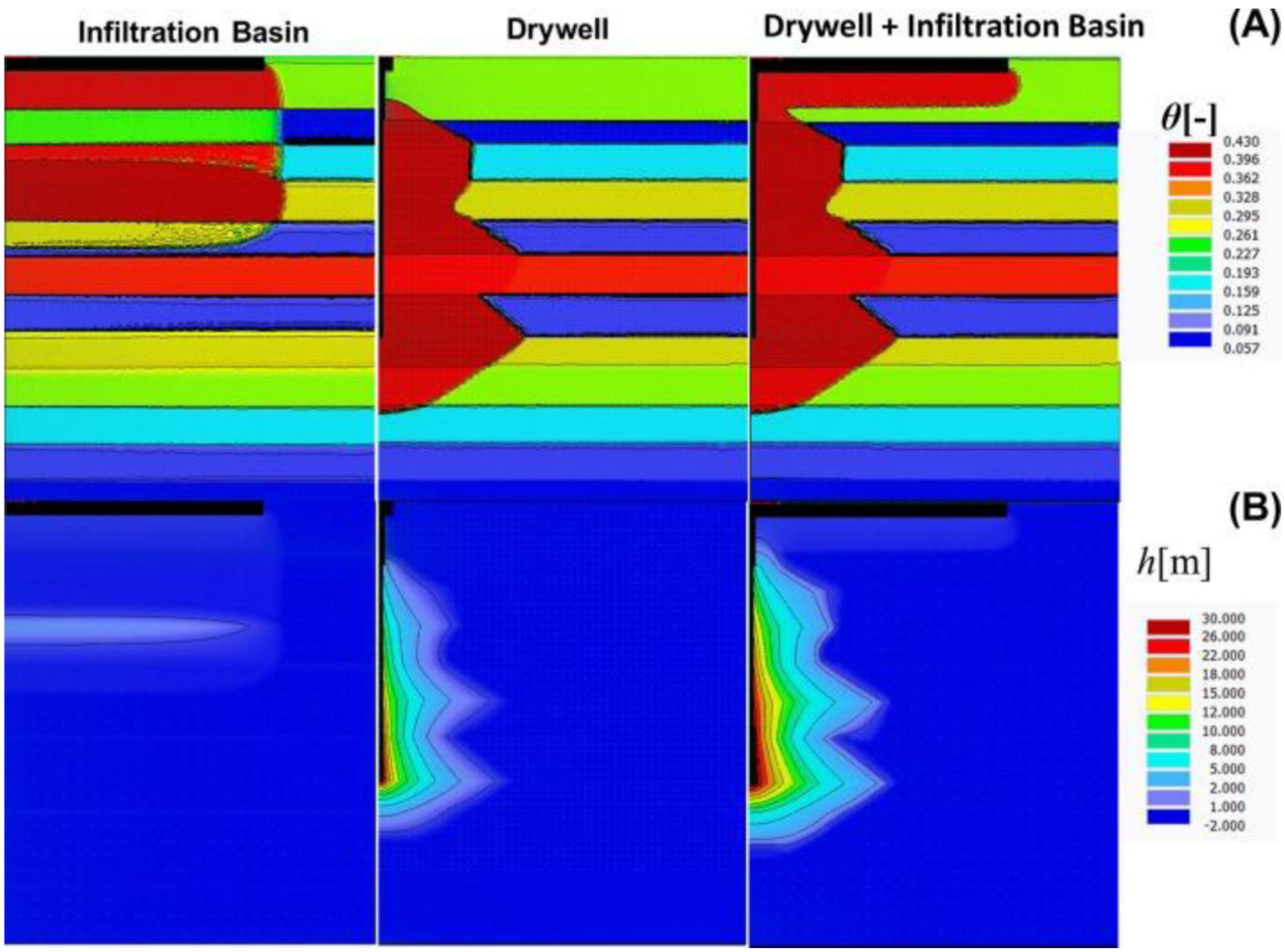

Fig. 9.

The water content (θ) (A) and pressure head (h) (B) profiles for a 70 m diameter infiltration basin, a DW, and a DW + an infiltration basin for a layered (Fig. S5) soil flow domain.

Table 1.

The soil hydraulic parameters for different soil materials employed in the numerical experiments.

Experiments	Soil	Domain	IB Size (Radius) [m]	Simulation Duration [minoryear]	Heterogeneity	Soil Hydraulic Parameters					
						θ_r^* [−]	θ_s^* [−]	α^* [m^{-1}]	n^* [−]	K_s^*[m day^{-1}]	l^* [−]
I	Fort Irwin Soil (Sasidharan et al., 2020)	Homogeneous	5 10 15 20 25 30 35 35	2 year	NA	0.043	0.39	9.17	2.76	0.046	0.5
II		Heterogeneous			X = 10; Z = 0.1; σ = 1 X = 1; Z = 0.1; σ = 1 X = 0.1; Z = 0.1; σ = 1 X = 1; Z = 1; σ = 1 X = 1; Z = 2; σ = 1 X = 1; Z = 0.1; σ = 0.5 X = 1; Z = 0.1; σ = 0.25						
III	Sand Loamy Sand Sandy Loam Sandy Clay Loam Clay			2014 min	Layered	0.045	0.43	14.5	2.68	7.13	0.5
						0.057	0.41	12.4	2.28	3.49	0.5
						0.065	0.41	7.5	1.89	1.06	0.5
						0.1	0.39	5.9	1.48	0.31	0.5
						0.068	0.38	0.8	1.09	0.048	0.5

*The residual soil water content (θr), the saturated soil water content (θs), the shape parameter (α), the pore-size distribution parameter (n), the saturated isotropic hydraulic conductivity (Ks), and the tortuosity parameter (l)